

N-87860

Technical Report No. 32-29

Launch-on-Time Analysis for Space Missions

C.E. Kohlhasse

FACILITY FORM 808

N66-83729	(THRU)
(ACCESSION NUMBER)	<i>none</i>
15	(CODE)
(PAGES)	
CR 94656	(CATEGORY)
(NASA CR OR TMX OR AD NUMBER)	



JET PROPULSION LABORATORY
CALIFORNIA INSTITUTE OF TECHNOLOGY
PASADENA, CALIFORNIA

August 15, 1960

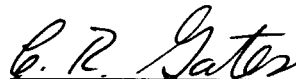


NATIONAL AERONAUTICS AND SPACE ADMINISTRATION
CONTRACT NO. NASW-6

Technical Report No. 32-29

Launch-on-Time Analysis for Space Missions

C.E. Kohlhasse

A handwritten signature in cursive script, reading "C. R. Gates", positioned above a horizontal line.

C. R. Gates, Chief
Systems Analysis

JET PROPULSION LABORATORY
CALIFORNIA INSTITUTE OF TECHNOLOGY
PASADENA, CALIFORNIA

August 15, 1960

CONTENTS

I. Introduction	1
II. Summary	1
III. Launching Azimuth	2
IV. Coast-Time Correction	6
V. Guidance Theory	8
VI. Results	9
Table 1. Launch-on-time results	9
Appendix	10
Nomenclature	11
References	12

FIGURES

1. Coordinate system and associated quantities	2
2. Launch site and vehicle coordinates	3
3. In-plane geometry	4
4. Effect of Earth rotation upon firing azimuth	5
5. Firing azimuth vs launch time for symmetric situation	5
6. Lunar coast-time correction geometry	6
7. Planetary coast-time correction geometry	6
8. Coast-time correction vs launch-time delay for symmetric situation	7
9. Powered-flight profile	8
A-1. Plumb-line coordinate system and associated quantities	10

I. INTRODUCTION

For lunar and planetary missions, it is desirable to formulate analytical methods for changing launch and powered-flight parameters in order to compensate for firing-time delays which may occur at the launching complex during an attempt to launch at a preselected standard firing time. Trajectory characteristics determine the amount of time delay that can be tolerated and therefore prescribe a "firing window," a time during which the vehicle may be launched without violating any of several constraints.

Parking-orbit trajectories (Ref. 1) will be discussed, as coast-time variation is a strong and essential parameter to control. In order to correct direct-ascent trajectories (Ref. 1) for launch-time delays, the vehicle generally must fly a steeper trajectory, which would result in undesirable performance.

This Report is designed to indicate the geometric aspects of the launch-on-time problem and to suggest how appropriate parameters might actually be controlled in order to effect a successful mission in the presence of firing-time delays.

II. SUMMARY

Various schemes might be adopted to handle the launch-on-time problem, but the ensuing discussion will be concerned with one particular method that has several desirable features. Equations will be presented which indicate how certain trajectory parameters must be changed in order to correct for launch-time errors. The method and associated equations, though not exact, are very good approximations which yield quite favorable results.

Firing azimuth and parking-orbit coast-time correction are the primary compensating parameters. After a launch-

time delay has occurred, the vehicle must be flown along a new or corrected launching azimuth. The vehicle is then guided to reobtain standard parking-orbit conditions. It should be noted here that use of the word "standard" throughout this Report will refer to available quantities associated with the standard, no-launch-time-error trajectory. Coast-time correction compensates for Earth rotation relative to the target. Final-stage burning is terminated when the vehicle achieves the standard injection energy (Ref. 1).

III. LAUNCHING AZIMUTH

The launching or firing azimuth σ_L is the angle measured clockwise from north to the projection of the missile thrust vector onto the local geodetic horizontal plane. It will be necessary to determine a new firing azimuth as a function of the launch-time delay Δt_L , so that the trajectory plane will contain the target at encounter. For lunar trajectories, this may be done by determining a launching azimuth such that the plane of motion defined at injection contains the position vector of the Moon defined at the time of expected lunar encounter. For interplanetary trajectories, the launching azimuth will be chosen so that the plane of motion defined at injection contains the asymptote to the standard departing hyperbola from Earth.

A. Nonrotating Spherical Earth

Consider the simple model of a nonrotating spherical Earth shown in Fig. 1. Let S represent a unit vector in the desired trajectory plane. In the case of lunar trajectories, S lies along the position vector of the Moon at the time of expected lunar encounter. The unit vector r , which points from the center of the Earth through the launching site, is given by

$$r = \cos \psi_L \cos \Theta_L i + \cos \psi_L \sin \Theta_L j + \sin \psi_L k \quad (1)$$

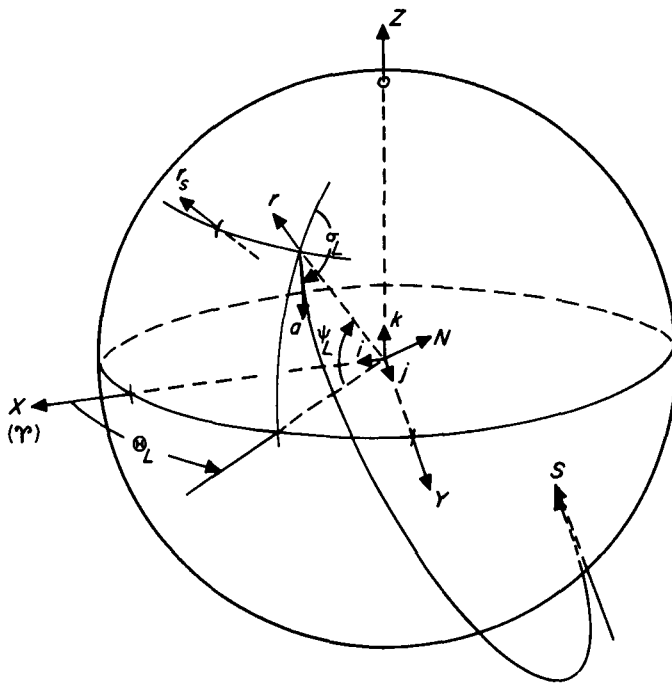


Figure 1. Coordinate system and associated quantities

where ψ_L and Θ_L are the geocentric latitude and right ascension of the launch site, and i, j, k are unit vectors defined by a space-fixed, equatorial, rectangular coordinate system with the X -axis towards the vernal equinox Υ . Right ascension is always measured in the equatorial plane, positive to the east, from the vernal equinox to the meridian of the point in question.

The unit vector a , pointing down the firing azimuth, is given by

$$a = \sec \psi_L \{ [k \times r] \sin \sigma_L - [(k \times r) \times r] \cos \sigma_L \} \quad (2)$$

It is now possible to determine the unit normal vector N to the plane of motion:

$$N = r \times a \quad (3)$$

$$\begin{aligned} N = & (\sin \Theta_L \cos \sigma_L - \cos \Theta_L \sin \psi_L \sin \sigma_L) i \\ & - (\cos \Theta_L \cos \sigma_L + \sin \Theta_L \sin \psi_L \sin \sigma_L) j \\ & + (\cos \psi_L \sin \sigma_L) k \end{aligned} \quad (4)$$

For a nonrotating, spherical Earth, the correct firing azimuth may be obtained by solving the equation $N \cdot S = 0$ for σ_L :

$$\sigma_L = \tan^{-1} \left[\frac{S_r \sin \Theta_L - S_\theta \cos \Theta_L}{(S_r \cos \Theta_L + S_\theta \sin \Theta_L) \sin \psi_L - S_z \cos \psi_L} \right] \quad (5)$$

B. Rotating Spherical Earth

The actual firing azimuth for a rotating Earth will, in general, lie slightly away from east of the azimuth given by Eq. 5. This deviation is essentially due to the initial crossrange-rate component, \dot{Z}_{L_0} , present at launch. Figure 2 displays an inertial, rectangular, launch-site coordinate system, defined at the instant of launch.¹ If expressions are developed for Z_L and \dot{Z}_L at injection, then the amount by which N has been rotated may be determined.

Parameters R , V , and Γ define vehicle position, inertial velocity, and path angle of the inertial-velocity vector. If drag is neglected and the assumption is made that vehicle thrust is maintained parallel to the $X_L Y_L$ plane, then

$$\ddot{Z}_L = - \frac{\mu}{R^2} \left(\frac{Z_L}{R} \right) \simeq - K Z_L \quad (6)$$

¹ Y_L is perpendicular to the spherical Earth model, X_L points along the downrange or azimuthal heading, and $Z_L = X_L \times Y_L$.

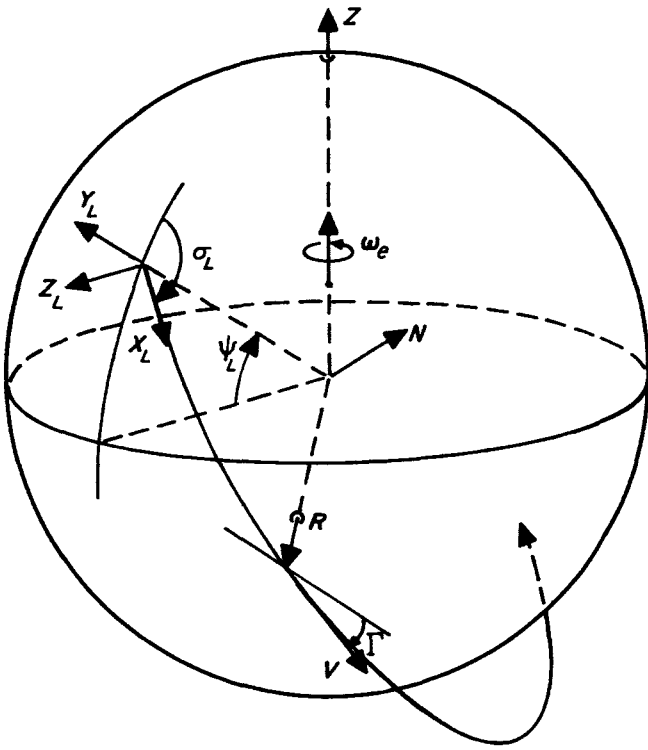


Figure 2. Launch site and vehicle coordinates

The subscript I refers to the values at injection, and the injection angular momentum C_{1I} is equal to $R_I V_I \cos \Gamma_I$. Equation 9 is a valid approximation, as ρ is a small rotation. In fact, for all firing azimuths within range-safety limits for the Atlantic Missile Range, the rotation does not exceed 0.05 rad.

Crossrange and crossrange rate were computed from Eq. 7 and 8 and compared with actual values obtained from an elaborate JPL powered-flight trajectory program. The comparison indicated an amplitude discrepancy and phase shift. The Appendix shows how this difficulty was partially eliminated by considering the plumb-line coordinate system that is actually used to define the standard vehicle thrust plane.

An observer located far above the launch site and looking in the $-Y_L$ direction would observe the trajectory curving to the right (for a southeast firing) as the vehicle accelerates downrange, after being launched with an eastward inertial velocity imparted by Earth rotation.

In order that the actual plane of motion defined at injection contain the desired S , it is necessary that

$$(N + \rho \times N) \cdot S = 0 \quad (10)$$

Solution of Eq. 10 for launching azimuth σ_L yields:

$$\sigma_L = \tan^{-1} \left\{ \frac{[S_x + S_y \rho_z - S_z \rho_y] \sin \Theta_L - [S_y + S_z \rho_x - S_x \rho_z] \cos \Theta_L}{[(S_y + S_z \rho_x - S_x \rho_z) \sin \Theta_L + (S_x + S_y \rho_z - S_z \rho_y) \cos \Theta_L] \sin \psi_L - [S_z + S_x \rho_y - S_y \rho_x] \cos \psi_L} \right\} \quad (11)$$

where K may be thought of as a time-averaged value of μR^{-3} over the powered flight from launch to injection. Integration of Eq. 6 leads to

$$\dot{Z}_L \simeq \dot{Z}_{L_0} \cos(K^{1/2} t) \quad (7)$$

$$Z_L \simeq K^{-1/2} \dot{Z}_{L_0} \sin(K^{1/2} t) \quad (8)$$

The initial crossrange-rate component \dot{Z}_{L_0} is equal to the product of the Earth's eastward surface velocity at the launch site and the cosine of the firing azimuth σ_L .

C. Rotation of Powered-Flight Plane of Motion

Imagine that the vehicle is flown to injection (for a nonrotating Earth) and then an instantaneous \dot{Z}_L is applied. This would have the effect of rotating the plane of motion defined at injection positively about R by an amount $-\dot{Z}_L (V \cos \Gamma)^{-1}$. The application of an instantaneous Z_L at injection would be equivalent to a rotation of the powered-flight plane about a line through the center of the Earth and parallel to V by an amount $Z_L (R \cos \Gamma)^{-1}$. It would therefore seem appropriate to define the rotation vector ρ :

$$\rho = C_{1I}^{-1} (Z_{L_I} V_I - \dot{Z}_{L_I} R_I) \quad (9)$$

Equation 11 refines Eq. 5 so as to include rotation of the powered-flight plane of motion. The right ascension of the launch site Θ_L is related to launch-time error Δt_L by:

$$\Theta_L = \Theta_{L_s} + \omega_e \Delta t_L \quad (12)$$

where Θ_{L_s} is the launch-site right ascension at the standard firing time and ω_e is the average angular velocity of the Earth.

D. Approximate Method for Obtaining Rotation Vector

The amount of rotation of the powered-flight plane of motion depends upon the launching azimuth. Neglecting oblateness, there would be no rotation for trajectories fired due east and maximum rotation for those launched due south. Therefore, in order to compute the firing azimuth from Eq. 11, ρ must be known; but, in order to determine ρ , the firing azimuth must be known. This situation may be handled without difficulty by first computing the firing azimuth from Eq. 5. The use of Eq. 5 for the computation is consistent with the assumption that the vehicle is flown to injection (for a nonrotating Earth) and that instantaneous Z_L and \dot{Z}_L are then applied

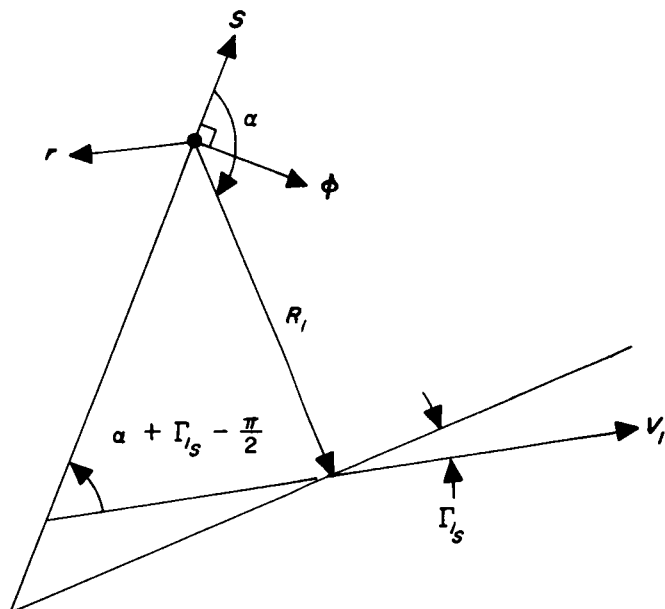


Figure 3. In-plane geometry

in order to determine the rotation of the powered-flight plane of motion.

The rotation vector \mathbf{p} depends upon C_{1p} , Z_{L_I} , V_I , \dot{Z}_{L_I} , and R_I ; C_{1p} is equal to the standard injection angular momentum, but something more must be said for the remaining quantities. In computing Z_{L_I} and \dot{Z}_{L_I} , the time from launch to injection t_I is given by

$$t_I = t_{I_s} + R_c V_c^{-1} [\cos^{-1}(\mathbf{r}_s \cdot \mathbf{S}_s) - \cos^{-1}(\mathbf{r} \cdot \mathbf{S})] \quad (13)$$

The first term on the right-hand side of Eq. 13 is the standard time from launch to injection, and the second term is the parking-orbit coast-time correction. The standard circular parking-orbit radius and velocity are R_c and V_c , respectively; \mathbf{r}_s is the unit position vector of the launch site at the standard launching time, and \mathbf{r} points through the launch site after the Earth has rotated to a new position which corresponds to the launch-time delay Δt_L . For lunar trajectories, \mathbf{S}_s and \mathbf{S} are, respectively, the unit position vectors of the Moon at the standard and launch-late times of expected lunar encounter. For interplanetary trajectories, $\mathbf{S}_s = \mathbf{S}$, a unit vector along the asymptote to the departing geocentric hyperbola. More will be said about the coast-time correction in Section IV.

Firing azimuth obtained from Eq. 5 is used to compute \dot{Z}_{L_0} so that, with Eq. 13, Z_{L_I} and \dot{Z}_{L_I} may now be determined for the launch-late trajectory. In order to determine R_I and V_I , it is assumed that the Earth is spherical and nonrotating and that injection occurs at the standard angle from \mathbf{S} . Figure 3 illustrates the in-plane geometry, where

$$\alpha = \cos^{-1} \frac{R_{I_s} \cdot \mathbf{S}_s}{R_{I_s}} \quad (14)$$

Equation 14 requires information available from the standard trajectory printout. Define a unit vector $\boldsymbol{\phi}$ normal to \mathbf{S} and given by

$$\boldsymbol{\phi} = \frac{(\mathbf{r} \cdot \mathbf{S}) \mathbf{S} - \mathbf{r}}{[1 - (\mathbf{r} \cdot \mathbf{S})^2]^{1/2}} \quad (15)$$

Should $\mathbf{a} \cdot \mathbf{S} > 0$, it will be necessary to use $(-\boldsymbol{\phi})$ defined by Eq. 15. Let $\Omega = \alpha + \Gamma_{I_s}$; then,

$$R_I = R_{I_s} [\cos \alpha \mathbf{S} + \sin \alpha \boldsymbol{\phi}] \quad (16)$$

$$V_I = V_{I_s} [\sin \Omega \mathbf{S} - \cos \Omega \boldsymbol{\phi}] \quad (17)$$

Now \mathbf{p} can be determined for use in Eq. 11. Figure 4 displays the amount by which the launching azimuth must be altered away from east in order to compensate for the eastward velocity of the launching site. The dashed curve obtained from Eq. 5 indicates launching azimuth for a typical lunar trajectory for various right-ascension or time locations of the launching site but assumes that, at the instant of launch, the Earth is nonrotating. The solid curve obtained from Eq. 11 gives the more accurate values of firing azimuth, as a function of the launch-time error, for a rotating Earth.

Figure 4 illustrates the effect of Earth rotation upon firing azimuth, but it provides only a fraction of the complete picture of firing-azimuth behavior with launch time. Imagine a situation defined by assuming $\Theta_{L_s} = 0$, $\psi_L = 30$ deg, and $\mathbf{S} = -(1 - S_z^2)^{1/2} \mathbf{i} + S_z \mathbf{k}$. This situation is described by Fig. 5, which indicates the variation of firing azimuth with launch time for several values of S_z . (Equation 5 was used to generate Fig. 5.) Although there are two possible firing azimuths for any given firing time, only the easterly values have been shown in Fig. 5. If ϕ represents the declination of \mathbf{S} , then $\phi = \sin^{-1} S_z$, and the curves of Fig. 5 may also be considered as curves of constant ϕ . The curves exhibit two characteristic patterns, with the critical boundary occurring at $|\phi| = |\psi_L|$. Note that for $|\phi| \leq |\psi_L|$, it is possible to fire at all azimuths (within range-safety limits). For $|\phi| > |\psi_L|$, a symmetric band of firing azimuths about due east is eliminated. Launch-on-time considerations generally favor launching when the rate of change of firing azimuth with launch is a minimum, if possible, as the associated firing windows are usually longer and the tracking geometry varies at the slowest possible rate. Accordingly, it is least desirable to launch when the $\partial \sigma_L / \partial t_L$ is very large.

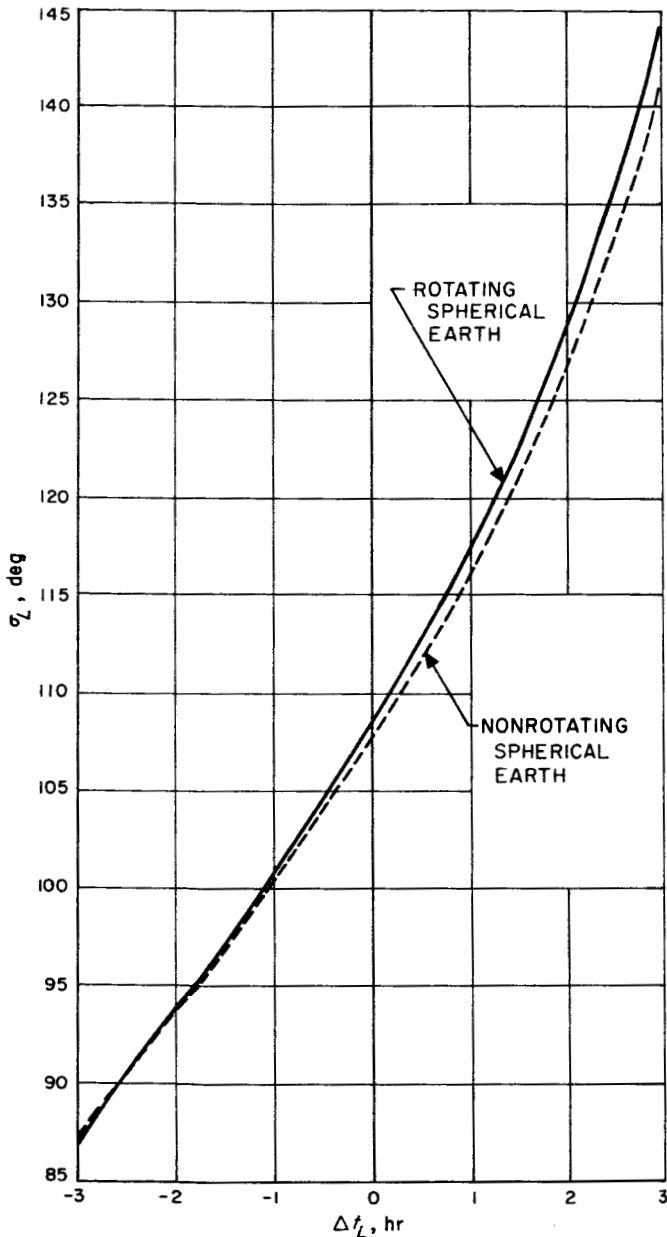


Figure 4. Effect of Earth rotation upon firing azimuth

In theory, there are always two possible firing azimuths for any given firing time. From a practical standpoint, range-safety restrictions for the Atlantic Missile Range may permit a band of firing azimuths from 46 to 114 deg east of north. Although some westerly firings are allowable from the Pacific Missile Range, they may well be undesirable in view of smaller payloads and inadequate tracking facilities. Presently, good tracking facilities exist for trajectories launched to the southeast from the AMR from about 95 to 110 deg. For most lunar and planetary missions, this would correspond to a practical firing window of between one and two hours.

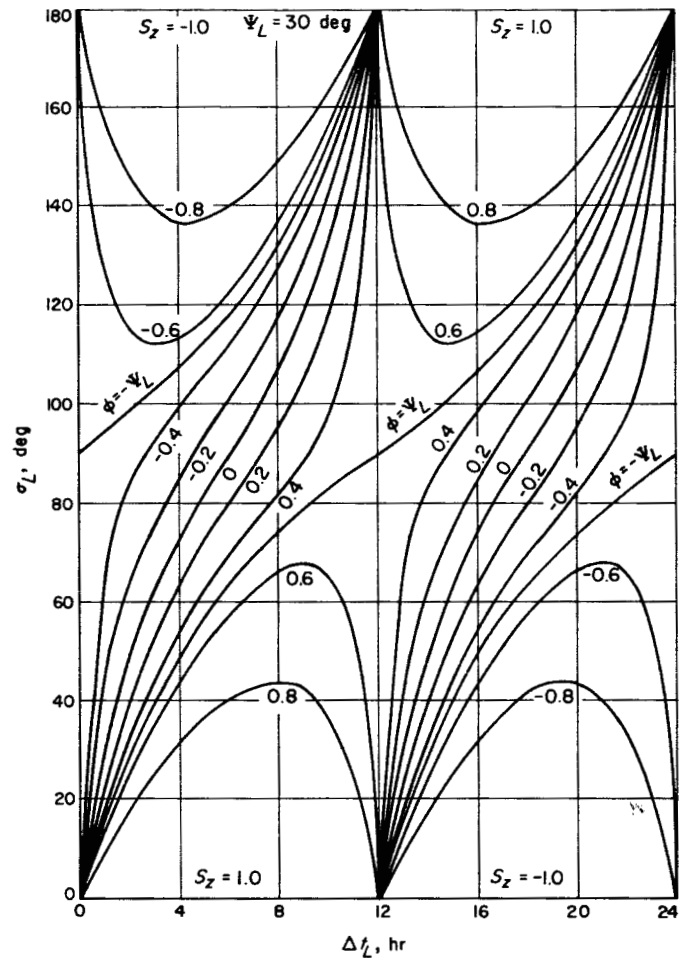


Figure 5. Firing azimuth vs launch time for symmetric situation

Although Fig. 5 illustrates firing-azimuth behavior with launch time for what appears to be a very special situation, it is actually representative of any real situation (for $\psi_L = 30$ deg) by a simple translation of the launch time axis. This is apparent when it is realized that any S vector may be expressed in the form assumed for Fig. 5 by performing an imaginary rotation of the equatorial coordinate axes in order to null S_y .

E. Taylor's Series Approximation

The correct launching azimuth may be obtained accurately for launch-time delays of less than half an hour or so by using the first three terms of a Taylor's series. For larger Δt_L , successive applications of Eq. 18 will suffice.

$$\sigma_L \simeq \sigma_{L_s} + \frac{\partial \sigma_L}{\partial t_L} \Delta t_L + \frac{1}{2} \frac{\partial^2 \sigma_L}{\partial t_L^2} \Delta t_L^2 \quad (18)$$

Relatively short expressions for the partial derivatives may be obtained readily from Eq. 5.

$$\frac{\partial \sigma_L}{\partial t_L} = \frac{\omega_e [(1 - S_z^2) \sin \psi_L - m S_z \cos \psi_L]}{n^2 + [m \sin \psi_L - S_z \cos \psi_L]^2} \quad (19)$$

where

$$m = S_x \cos \Theta_{L_s} + S_y \sin \Theta_{L_s}$$

$$n = S_x \sin \Theta_{L_s} - S_y \cos \Theta_{L_s}$$

Note that whenever $m = S_z^{-1}(1 - S_z^2) \tan \psi_L$ and the denominator of Eq. 19 is non-zero, the rate of change of firing azimuth with respect to launch time is zero. Given that $|\phi| > |\psi_L|$, it is possible to determine the firing time associated with the flat portion of the curves of Fig. 5.

Differentiating again with respect to launch time,

$$\frac{\partial^2 \sigma_L}{\partial t_L^2} = n D^{-1} S_z \omega_e^2 \cos \psi_L - 2 \omega_e N D^{-2} \times [m n \cos^2 \psi_L + n S_z \sin \psi_L \cos \psi_L] \quad (20)$$

where N and D are the numerator and denominator of Eq. 19.

Finally, the most accurate method for computing the correct launching azimuth would be to evaluate the partial derivatives from Eq. 11. In this way, the change in the amount of rotation of the powered-flight plane of motion, with changing launch azimuth, would be included. This effect is shown by Fig. 4. Note how the two curves slowly diverge as the firing azimuth swings away from east. Several long equations (not presented in this Report) are generated by differentiating Eq. 11 with respect to launch time.

IV. COAST-TIME CORRECTION

A parking-orbit coast-time correction Δt_c must be made in order to compensate for Earth rotation relative to the prescribed asymptote S . Note in Fig. 1 how the in-plane angle from launch to the asymptote diminishes as the launch site moves from r_s to r . For lunar trajectories, this effect is illustrated in Fig. 6, where the standard and launch-late planes of motion are shown coplanar, in order to illustrate the in-plane geometry. The coast-time correction is therefore given by

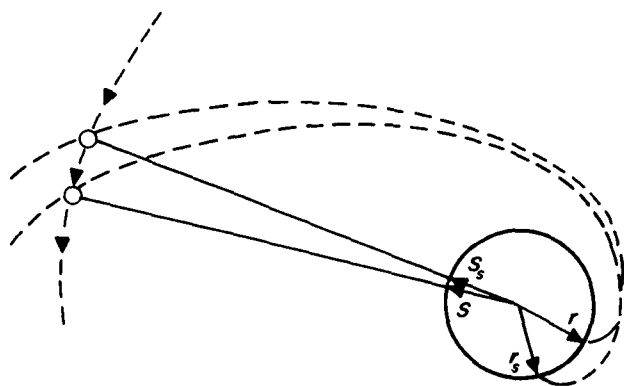


Figure 6. Lunar coast-time correction geometry

$$\Delta t_c = R_c V_c^{-1} [\cos^{-1}(r_s \cdot S_s) - \cos^{-1}(r \cdot S)] \quad (21)$$

All quantities in Eq. 21 have been previously defined in Section III-D. Should $a \cdot S > 0$ for r_s and r , it is necessary to use $-\Delta t_c$ as defined by Eq. 21.

Figure 7 illustrates the geometry for interplanetary trajectories. Note that $S = S_s$, the asymptote to the stand-

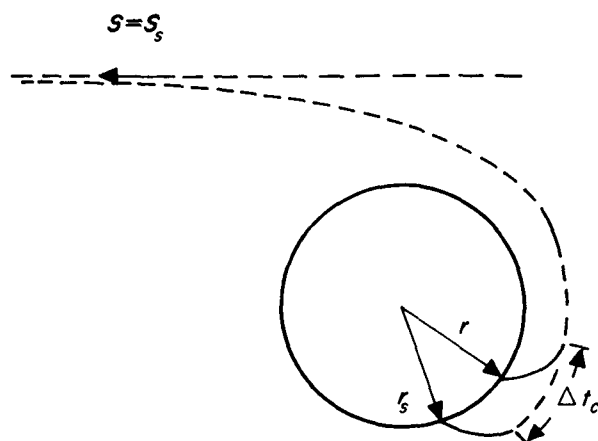


Figure 7. Planetary coast-time correction geometry

and departing geocentric hyperbola. Strictly speaking, the exact choice for S should be slightly different from S_s , as the heliocentric geometry has undergone a very small change after the passage of a launch-time delay. However, since the purpose of this Report is to obtain good analytical approximations, no exact analysis will be conducted here in order to arrive at a better choice for S .

Note that Eq. 21 could easily be mechanized to compute Δt_c as a function of Δt_L . For interplanetary trajectories, the only variable on the right-hand side of the equation is r , which is certainly a function of Δt_L . For lunar trajectories and launch-time delays that do not exceed a few hours, S varies approximately as

$$S \simeq \frac{R_{m_s} + \Delta t_L V_{m_s}}{|R_{m_s} + \Delta t_L V_{m_s}|} \quad (22)$$

where R_{m_s} and V_{m_s} are the geocentric position and velocity of the Moon at the standard time of lunar encounter. Equation 22 assumes that, since the standard injection energy is maintained, the flight time from injection to encounter does not significantly change for nominal launch-time delays. It also neglects Δt_c , which is small in comparison to Δt_L .

Figure 8 illustrates coast-time correction (based upon a 100-nautical-mile circular parking orbit) vs launch time for the symmetric situation described by Figure 5. The discontinuity at $\Delta t_L = 12$ results from considering only the easterly launching azimuths ($0 \leq \sigma_L \leq 180$ deg). Figure 8 also assumes that whenever the downrange angle from r to S is less than 180 deg, then the vehicle must coast around the Earth before departure. The value of this minimum downrange angle is dependent upon the type of vehicle and the particular mission (Ref. 1). For many of the current vehicles and anticipated missions, this angle may vary from about 150 to 200 deg, and 180

deg was merely chosen as a typical value. For all possible parking-orbit trajectories, $0 \leq |\partial t_c / \partial t_L| \leq \omega_e R_c V_c^{-1}$. Typically, $\partial t_c / \partial t_L \simeq -0.05$ about the nominal firing time for many of the envisaged space missions that employ the parking-orbit technique.

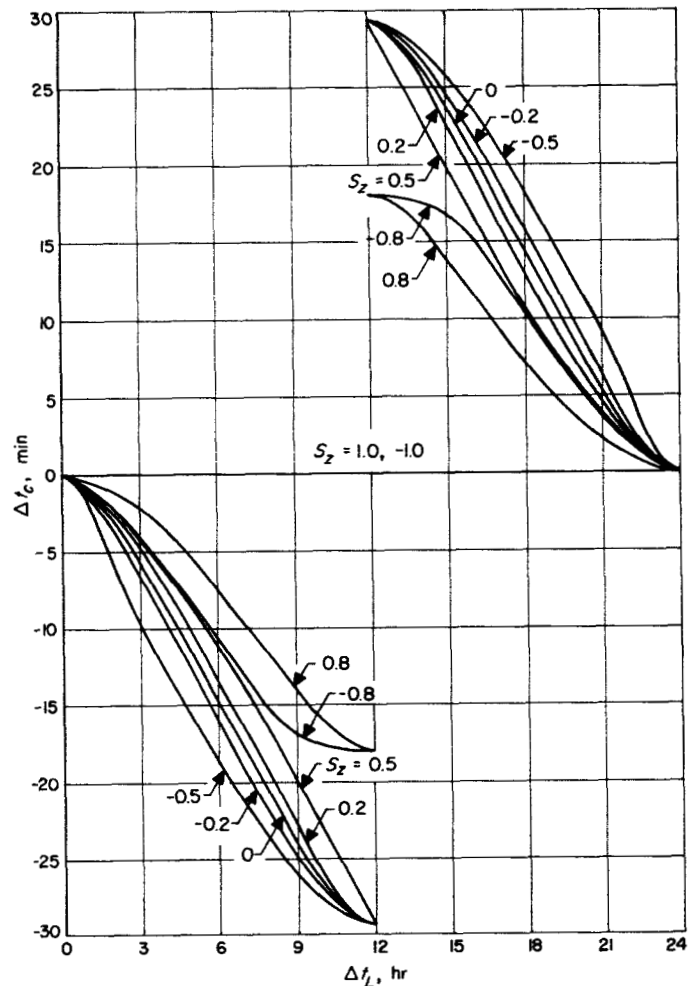


Figure 8. Coast-time correction vs launch-time delay for symmetric situation

V. GUIDANCE THEORY

Consider, for the sake of discussion, a two-stage vehicle with second-stage restart capability. Figure 9 shows the in-plane points of interest for a typical powered-flight trajectory from launch to injection.

With the occurrence of a launch-time delay, a new firing azimuth and coast-time correction would be obtained and relayed to the vehicle guidance system. The vehicle would rise vertically from the launching pad and perform a roll maneuver in order to arrive at the desired azimuthal heading, before initiating a preset pitch program designed to control the vehicle until aerodynamic effects had become negligible. The remaining portion of the first stage could then be guided either inertially or by radio command. Yaw-error guidance might be accomplished by nulling a signal proportional to $\mathbf{R} \times \mathbf{V} \cdot \mathbf{S}$. Pitch guidance could steer the vehicle to attain the standard value of angular momentum when a shutoff signal terminates first-stage burning upon reaching the standard energy.

After a short coasting period, the second stage would be ignited and guided to achieve the standard circular parking-orbit altitude and velocity. In addition to the coast-time correction for launch-time delay, an adjustment would be made to the second-stage restart time in order to compensate for downrange errors arising from performance dispersions prior to parking-orbit entry.

The final injection phase would place strict require-

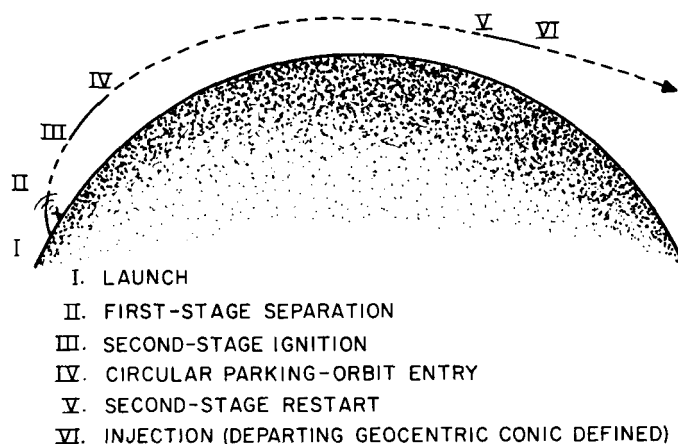


Figure 9. Powered-flight profile

ments on the guidance system (Ref. 2). Yaw guidance would still control the plane of motion to contain \mathbf{S} . In spite of position dispersions about the injection point, pitch guidance would control the inertial path angle Γ to maintain the desired asymptote. Final engine shutoff would be commanded when, for example, $V^2 - 2\mu R^{-1}$ reached the standard value of twice the total energy-per-unit mass. The injection conic has now been defined. Radio tracking data could be used to determine a mid-course maneuver (Ref. 3), necessary to correct for injection deviations which may have arisen from component and other possible error sources.

VI. RESULTS

The equations given in this Report are designed to indicate an approximate method for handling the launch-on-time problem. Three representative standard trajectories were chosen to evaluate the effectiveness of this method. Equations 18, 19, and 20 were used to compute firing azimuth, and the coast-time correction was determined from Eq. 21. Table 1 illustrates the performance of the corrective equations. An elaborate JPL trajectory program provided the standard and launch-late trajectories. The unusually small firing-azimuth change for the Mars trajectory resulted because the $\partial\sigma_L/\partial t_L$ was nearly zero for this particular standard Mars asymptote and launching time.

The miss distances could have been further reduced, had Eq. 18 been successively applied with smaller Δt_L , and had the more exact partials been substituted in the Taylor's series expansion for computing firing azimuth. The miss distances shown in Table 1 are considerably smaller than those which arise from component-error sources in present injection-guidance systems.

Accurate digital-computer programs may be used to obtain exact trajectories for the limiting firing azimuths associated with a given firing window. If desired, one or two additional trajectories might also be obtained within the window. Corrective equations could then be used with the vehicle guidance system to provide the capability for continuous firing within the given window.

Table 1. Launch-on-time results

Key parameters	66-hour lunar	66-hour lunar	176-day Mars
Launch-time delay, min	60	60	30
Launching-azimuth change, deg	108.0 → 116.8	96.0 → 105.0	112.0 → 112.9
Coast-time correction, sec	-175.9	-185.3	-90.1
Miss distance from target center with no correction for launch time delay, mi	4.90×10^4	4.60×10^4	4.87×10^6
Miss distance from target center with corrective equations but no mid- course maneuver, mi	190 (impact)	350 (impact)	1.60×10^4

APPENDIX

Realistic Crossrange and Crossrange Rate

Figure A-1 depicts an inertial plumb-line coordinate system, defined at the instant of launch. A plumb line suspended at the launching site would lie along Y_p . The downrange or azimuthal heading is defined by X_p , and $Z_p = X_p \times Y_p$. The standard vehicle thrust plane is maintained parallel to the X_p, Y_p plane. In Fig. A-1, X_p, Y_p, Z_p has been translated to the center of the Earth and designated X'_p, Y'_p, Z'_p .

Assuming, as in Section III-B, that $\ddot{Z}'_p \simeq -KZ'_p$,

$$\dot{Z}'_p \simeq \lambda A \cos(\lambda\beta + K^{1/2}t) \quad (A-1)$$

$$Z'_p \simeq K^{-1/2} A \sin(\beta + \lambda K^{1/2}t) \quad (A-2)$$

where

$$A = (\dot{Z}'_{p0}{}^2 + KZ'_{p0}{}^2)^{1/2} \quad (A-3)$$

$$\dot{Z}'_{p0} = v_L \cos \sigma_L \quad (A-4)$$

$$Z'_{p0} = R_0 \sin \sigma_L \sin(\psi_p - \psi_L) \quad (A-5)$$

$$\beta = \sin^{-1}(K^{1/2} A^{-1} Z'_{p0}), \quad -\frac{\pi}{2} \leq \beta \leq \frac{\pi}{2} \quad (A-6)$$

$$K = \mu R^{-3} \quad (A-7)$$

$$\lambda = \begin{cases} 1, & \dot{Z}'_{p0} \geq 0 \\ -1, & \dot{Z}'_{p0} < 0 \end{cases} \quad (A-8)$$

When compared with the actual values obtained from the JPL powered-flight trajectory program, \dot{Z}'_p and Z'_p , computed from Eq. A-1 and A-2, still indicated a slight amplitude error and phase shift. This discrepancy resulted from the basic assumption that $\ddot{Z}'_p \simeq -KZ'_p$, which neglected the oblateness of the Earth by assuming that the gravitational force was directed towards the Earth's center.

In comparing the actual with the computed curves of crossrange and crossrange rate for trajectories launched at different azimuths from the Atlantic Missile Range, it was found that excellent agreement (over the initial portion of flight through in-plane angles less than about 30 deg) could be realized by using an initial crossrange

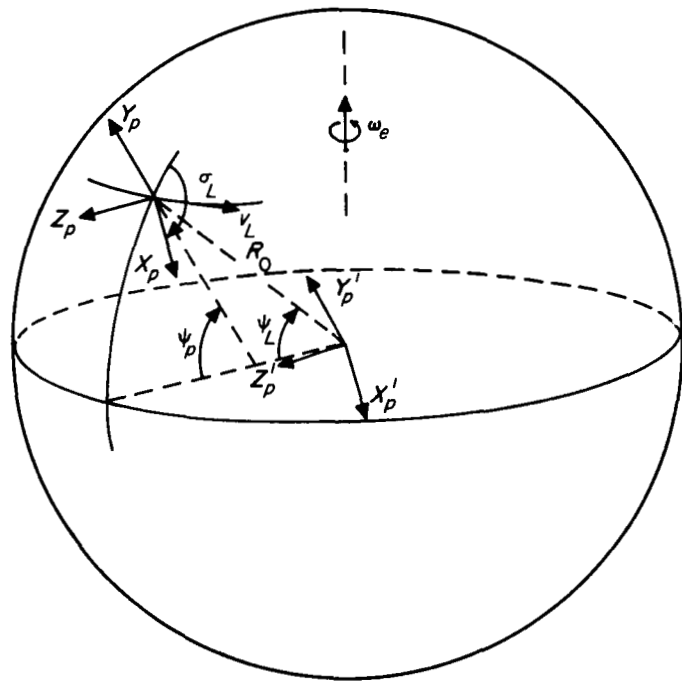


Figure A-1. Plumb-line coordinate system and associated quantities

displacement of approximately half that given by Eq. A-5. This result is suggested by the nearly equal contributions to $(\psi_p - \psi_L)$ from the gravitational and centrifugal forces associated with a rotating, oblate Earth.

It should be remembered that the reason for obtaining crossrange and crossrange-rate expressions was to determine the amount and direction of rotation of the launch-to-injection plane of motion. This rotation was then used to refine the firing azimuth calculation. An analysis of the effect of oblateness upon crossrange and crossrange rate will not be presented here. Such an analysis, if conducted, would indicate a dependence of A , β , and K upon the oblateness expression (Ref. 4). The amount of rotation of the powered-flight plane of motion can be obtained with acceptable accuracy without resorting to a cumbersome analysis involving the detailed effects of oblateness.

NOMENCLATURE

a	unit vector having direction of vehicle-thrust-vector projection in local horizontal plane at launch (direction defined by σ_L)	Z_p, \dot{Z}_p	actual vehicle crossrange and crossrange rate
C_1	angular momentum defined by $RV \cos \Gamma$	A	amplitude function representing maximum crossrange rate
C_3	twice total energy-per-unit mass $= V^2 - 2\mu R^{-1}$	β	phase angle arising from initial crossrange displacement
K	time-averaged value of μR^{-3} over powered flight from launch to injection	Γ	angle from local horizontal plane to inertial velocity vector
N	unit vector normal to vehicle thrust plane defined at launch	Δt_c	parking-orbit coast-time correction
R	position vector of vehicle	Δt_L	launch-time error (positive for a late launch)
R_c	circular parking-orbit radius	Θ_L	right ascension of launch site
R_{m_s}	position vector of Moon at time of expected lunar encounter for standard trajectory	μ	gravitational constant for Earth (GM_e)
R_0	Earth radius at launching site	ρ	rotation vector of powered-flight plane of motion
r	unit vector pointing from center of Earth through launching site	σ_L	launching azimuth; prescribes orientation of vehicle thrust vector as measured clockwise from north
S	unit vector along asymptote to geocentric hyperbola for interplanetary trajectories; lies along lunar position vector at time of expected encounter for lunar trajectories	ϕ	declination of S
V	inertial velocity vector of vehicle	Φ	unit vector normal to S and in plane of motion (see Fig. 3)
V_c	circular parking-orbit velocity	ψ_p	geodetic latitude of launch site
V_{m_s}	lunar velocity relative to Earth's center at standard time of expected lunar encounter	ψ_L	geocentric latitude of launch site
v_L	Earth-surface velocity at launching site	ω_e	average angular velocity of Earth
X, Y, Z	space-fixed, equatorial coordinate system with X -axis toward vernal equinox; prescribes unit vectors i, j, k (see Fig. 1)	Subscripts	
X_L, Y_L, Z_L	inertial launch-site coordinate system, defined at instant of launch (see Fig. 2)	c	circular parking-orbit conditions
X_p, Y_p, Z_p	inertial plumb-line coordinate system, defined at instant of launch (see Fig. A-1)	I	parameter values at injection
Z_L, \dot{Z}_L	vehicle crossrange and crossrange rate for simplified mathematical model of Fig. 2	L	launch site
		m	lunar quantities
		p	plumb-line coordinates
		s	values associated with standard, no-launch-time-error trajectory
		x, y, z	values associated with X, Y, Z coordinate system (Fig. 1)
		0	initial value of a given parameter

REFERENCES

1. Clarke, V. C., Jr. Design of Lunar and Interplanetary Ascent Trajectories. Pasadena, Calif., Jet Propulsion Laboratory, California Institute of Technology, July 26, 1960. (TR 32-30)
2. Pfeiffer, C. G. Guidance for Space Missions. Pasadena, Calif., Jet Propulsion Laboratory, California Institute of Technology, June 12, 1959. (EP 656)
3. Noton, A.R.M., Cutting, E., and F. L. Barnes. Analysis of Radio-Command Mid-Course Guidance. Pasadena, Calif., Jet Propulsion Laboratory, California Institute of Technology, September 8, 1960. (TR 32-28)
4. Jeffreys, H. The Earth, 4th edition. Cambridge, Cambridge University Press, 1959.